

Correlating quantitative magnetization transfer (qMT) and diffusion tensor imaging (DTI) with myelin histology in a rat model of type III multiple sclerosis (MS) lesions

Vaibhav Anil Janve^{1,2}, Zhongliang Zu¹, Song-yi Yao³, Ke Li¹, Fang Lin Zhang³, Kevin Wilson¹, Xiawei Ou⁴, Mark Does^{1,5}, Subramaniam Sriram³, and Daniel Gochberg^{1,2}

¹Institute of Imaging Science, Vanderbilt University, Nashville, TN, United States, ²Department of Physics, Vanderbilt University, Nashville, TN, United States, ³Department of Neurology, Vanderbilt University School of medicine, Nashville, TN, United States, ⁴Department of Radiology, Arkansas Children's Hospital, ⁵Radiology and Radiological Sciences, Vanderbilt University

Introduction:

Demyelination is a feature of many white matter diseases, such as multiple sclerosis (MS), and quantifying the extent of demyelination has important clinical implications in monitoring disease progression, treatment planning, and drug response. Quantitative MRI methods including quantitative magnetization transfer imaging (qMT) and diffusion tensor imaging (DTI) have been shown to be sensitive to demyelination [1,2]. However these methods are based on different physical principles and are indirectly related to myelin content. Correlating quantitative metrics obtained from these methods with quantitative histological measures of myelin content may reveal their relative sensitivity and specificity towards demyelination. In this study, we present correlation of high-resolution 3D qMT and DTI matrices (167 μ m isotropic) with reconstructed quantitative 3D Luxol fast blue-periodic acid Schiff (LFB-PAS) stained histological volume in a lipopolysaccharide (LPS) mediated animal model of MS. Injection of LPS into the central nervous system (CNS) results in an acute inflammatory response followed by demyelination that is typical of a progressive oligodendroglialopathy [3, 4]. We seek to develop an animal model system of Type III oligodendroglialopathy that reflects the apoptotic death of oligodendrocytes which is seen in the relative absence of prominent lymphocytic infiltration. To our knowledge this is the first quantitative magnetic resonance myelin study of an animal model of Type III MS lesions.

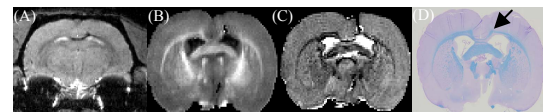


Fig. 1 Representative (A) *in vivo* T2* weighted 3D gradient echo image, (B) PSR map, (C) RD map (D) LFB-PAS stained histology slice, containing injection site.

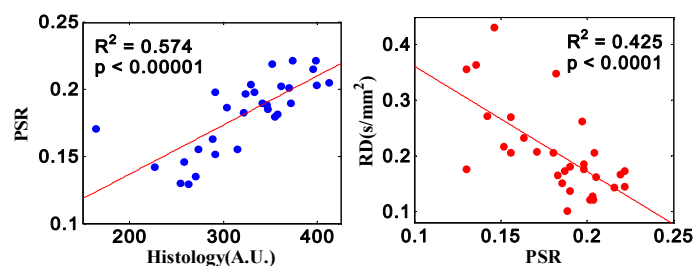


Fig.2 Scatter plots from single rat. Each point represents a 1mm section of CC in one of the 5 slices near injection site (a) PSR vs LFB histology, (b) RD vs PSR.

Following *in vivo* imaging the rat brains were perfusion fixed with formalin fixative and *ex vivo* 3D high resolution (167 μ m isotropic) qMT and DTI scans were performed on the perfusion fixed brains. The qMT scans were performed using an optimized selective inversion recovery method [6, 7]. DTI scans were performed using 3D PGSE, 6(+1) directions with bvalue 1200s/mm², TE/TR=29/250 ms, in 8.5hrs. **Histopathology:** 4mm coronal tissue sections containing the site of injection were excised, blocked in paraffin, sectioned in 10 μ m slices, stained with Luxol fast blue (LFB) or Luxol fast blue-periodic acid Schiff (LFB-PAS), and quantified by optical opacity. **Data analysis:** For one rat a 3D histological image volume was created by co-registering each LFB slide image to its neighboring slide sampled to match the *ex vivo* MR resolution of about 167 μ m. This volume was then co-registered to the *ex vivo* 3D MR images for quantitative analysis. Co-registration was performed using rigid and affine registration programs maximizing the mutual information. Six 1mm ROIs were segmented within the CC for 5 slides containing the injection site, giving a total of 30 ROIs for analysis. For all other samples a single slice containing the site of injection was matched with registered MRI data and three 1mm ROI's were selected on either side of the midline in the CC, giving a total of 6ROI's for each sample. **Statistical analysis:** Pearson's correlation coefficients were calculated using mean ROI values for MR and histological matrices.

Results and Discussion:

LFB/LFB-PAS staining confirmed demyelination in proximity of the injection site in CC of LPS injected rats. Histological measure of myelin content, as well as qMT and DTI parameters, show variation within the white matter in CC. Saline injected rats showed demyelination, however the chances of occurrence were significantly lower than in LPS injected rats. Correlations are observed within the CC between histological measure of myelin content and qMT and DTI metrics (See Fig 2 for example 3D results and Fig 3A for correlation summaries of all 2D rat studies). Apparent pool size ratio (PSR) shows the largest positive correlation with histological measure of myelin content, while DTI measured radial diffusivity (RD) shows the largest negative correlation. RD is also negatively correlated to PSR (Fig 3B). Weaker correlations to LFB were observed for other parameters including rate of magnetization transfer from macromolecular to free proton pool (k_{mf}), DTI measured fractional anisotropy (FA), and axial diffusivity (AD). These preliminary results indicate a strong correlation between histological measure of myelin and PSR and RD (and to lesser extent R1f, FA, and AD) across LPS injected rat in the CC, indicating that these measures may provide a sensitive measure of demyelination.

References:

1) Song SK et al, Neuroimage 26 (2005) 132-140 2) Underhill HR et al. Neuroimage 54(2011)2052-2065 3) Felts PA et al, Brain 128, 1649-1666 (2005), 4) Lucchinetti C et al, Ann Neurol 47, 707-17(2000), 5) H.E. D'Arceuil et al. Neuroimage 35 (2007) 553-565 6) Gochberg DF et al, MRM 2007:57:437-441. 7) Li K et al. MRM 2010:64: 491-500.

Acknowledgements:

This research is supported by NIH R01EB001452 and Vanderbilt Bridge Funding grants.

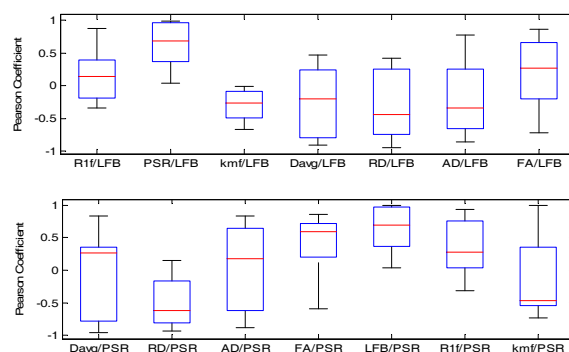


Fig.3 Box plot summary of Pearson coefficients for 9 (7 LPS, 2 Ctrl) rats (A) qMT and DTI metrics vs LFB histology, (B) qMT and DTI metrics vs PSR. The box has lines at the lower quartile, median, and upper quartile values with error bars covering the complete range.